

TERAHERTZ RADIATION DOI: 10.1070/QEL16098

Optical-to-THz radiation conversion on a semi-metal surface

V.A. Mironov, I.V. Oladyshkin, D.A. Fadeev

Abstract. **We consider the possibility of generation of broadband terahertz (THz) radiation upon reflection of a p-polarised femtosecond laser pulse from the surface of a semi-metal. The hydrodynamic model of an instantaneous quadratic response of metals is generalised, and analytical results and numerical simulation data are presented. It is shown that transition from highly conductive metals to semi-metals is accompanied by a significant increase in the efficiency of the THz signal generation due to the reduction of the effective charge carrier mass and attenuation of the shielding of optical and THz fields.**

Keywords: *semi-metal, terahertz radiation, femtosecond laser pulses, nonlinear optics.*

1. Introduction

Active mastering of the terahertz (THz) range of electromagnetic waves has led to a marked development of the physics of nonlinear conversion of optical radiation into low-frequency radiation. In particular, at present, much attention is paid to the experimental and theoretical research of THz radiation generation in the interaction of femtosecond laser pulses with surfaces of metals and other conductive media [1–9]. A detailed study of THz radiation generation upon its reflection from the boundary of a medium is aimed not only at enhancing the optical-to-terahertz conversion efficiency, but also at investigating, in conjunction with other electrodynamic methods (generation of surface waves, harmonics of optical fields, etc. [10, 11]), the material itself [12].

Properties of THz generation upon reflection of femtosecond pulses from highly conductive metal surfaces (gold, copper, aluminium, etc.) have been studied in sufficient detail [1–9, 12]; generation efficiency at typical experimental parameters is low, on the order of 10^{-7} (with respect to energy). Theoretical papers [7, 8] show that the low efficiency of conversion of laser pulses is associated with a high concentration of free charge carriers: volume currents in a dense plasma almost completely shield radiation of a nonlinear surface current.

The aim of this paper is to draw attention to a new class of materials, i.e. semi-metals. Below, we will generalise the hydrodynamic model of THz generation, developed in [5, 7, 8], to the case of semi-metals, which have a relatively small concentration of electrons in the conduction band. For an instantaneous quadratic response of such a medium to be obtained, it is fundamentally important to take into account interband transitions and significant anisotropy of the effective masses of charge carriers.

The paper presents analytical results and provides numerical simulation data within the framework of the full hydrodynamic model. We present a comparative evaluation for base metals and bismuth, whose linear electrodynamic characteristics are experimentally investigated in detail over a wide frequency range [13–15]. It is shown that the transition from metal to semi-metals is accompanied by a marked increase in the efficiency of THz generation due to an instantaneous quadratic response of electrons. In addition, in accordance with the developed THz model, the bismuth response is expected to be sensitive to the orientation of a single-crystal sample due to a strong anisotropy of the electron effective mass tensor. Thus, the optical-to-THz-radiation conversion on surfaces of semi-metals may be of interest from the standpoint of the study of their electromagnetic characteristics.

In Section 2 we describe the characteristics of incident and reflected laser radiation within the framework of the linear model. The basic expressions presented there are used in Section 3 to derive a relationship for a longitudinal surface current, which is induced by a laser pulse at the sample surface. In Section 4 we consider the problem of an electromagnetic pulse generated by a surface current source moving along the surface with a phase velocity exceeding the speed of light in vacuum. Concluding remarks are given in Section 5. In the Appendix, we present clarifying information about the numerical methods used, with reference to the previous work.

2. Reflection of a laser pulse from the surface of a semi-metal

Let us consider a semi-metal sample on the surface of which monochromatic p-polarised optical radiation is incident. We introduce a coordinate system by directing the z axis along the surface in the plane of incidence, the x axis perpendicular to the surface, and the y axis perpendicular to the plane of incidence. Because the real part of the dielectric constant ε at optical frequencies is large in absolute value and negative [15], the electric field E decreases exponentially inside of the sample:

$$E_x = E_{x0}\exp(k_0\sqrt{-\varepsilon}\,x - \mathrm{i}k_0 z\cos\alpha), \quad (1)$$

$$E_z = E_{z0}\exp(k_0\sqrt{-\varepsilon}\,x - \mathrm{i}k_0 z\cos\alpha), \quad (2)$$

V.A. Mironov, I.V. Oladyshkin, D.A. Fadeev Institute of Applied Physics, Russian Academy of Sciences, ul. Ulyanova 46, 603950 Nizhnii Novgorod, Russia; e-mail: oladyshkin@gmail.com

Received 30 March 2016; revision received 21 June 2016
Kvantovaya Elektronika **46** (8) 753–758 (2016)
Translated by I.A. Ulitkin

where the angle of incidence α is measured from the z axis; $k_0 = \omega_0/c$ is the wave number of optical radiation in vacuum; and E_{x0} and E_{z0} are the wave amplitudes at the sample boundary. The reflection coefficient R can be represented as follows [16]:

$$R = \frac{\varepsilon \sin\alpha - \sqrt{\varepsilon}}{\varepsilon \sin\alpha + \sqrt{\varepsilon}}. \tag{3}$$

Interference of incident and reflected waves leads to the fact that near the interface between two media ($x = 0$), the total field propagates along the surface with a phase velocity greater than the speed of light (see details in [7]). Thus, if the laser pulse length is sufficiently small compared to its transverse dimensions, a superluminous light spot is formed in the region of the overlap of incident and reflected optical radiation. As will be shown below, a low-frequency nonlinear current can be excited in this spot on the surface of the semimetal. Therefore, we need to generalise the electrodynamic model of the medium in order to determine this current.

The dielectric constant of bismuth is fairly well studied experimentally and interpreted theoretically [13, 14]. It is determined by the polarisation response of the crystal lattice, as well as by interband transitions and intraband electron motion. Below, we will use the phenomenological model of the linear response that contains only a small number of parameters. In their determination, we will focus on the experimentally observed dependence of the dielectric constant of bismuth on the frequency in the region under consideration [15]. The intraband motion of holes will not be taken into account in the derivation of the polarisation response, since their effective mass is much greater than the mass of the electron.

The polarisation response of bismuth has a resonance behaviour near the frequency $\omega_b \sim 10^{15}$ s^{-1}, caused by transitions of electrons from the filled valence band or from the conduction band to the empty zone lying above (the characteristic difference between the energies is 1–0.7 eV). We take into account this contribution by using a harmonic oscillator model to describe the dynamics of the medium polarisation:

$$\ddot{P} + \nu_b \dot{P} + \omega_b^2 P = \beta E(t), \tag{4}$$

where ω_b is the eigenfrequency of the oscillator; P is the polarisation of the medium; ν_b is the effective loss rate; β is the coupling coefficient; $E(t)$ is the electric field; and the dot above the letter denotes differentiation with respect to time.

The motion of particles in the conduction band can be described based on the model of free electrons:

$$\ddot{\boldsymbol{r}}_f = -\nu_f \dot{\boldsymbol{r}}_f - e\hat{M}_f^{-1}\boldsymbol{E}, \tag{5}$$

where r_f is the classical electron coordinate; e is the electron charge; $\hat{M}_f$ is the tensor of the effective mass of a free electron; and ν_f is the effective collision frequency. The polarisation response associated with the intraband motion of electrons will be important below for obtaining a nonlinear current. Below we consider an optical field, polarised in the xz plane, by assuming that the corresponding sub-matrix $\hat{M}_f$ is diagonal and has diagonal components m_x and m_z. In the case of bismuth, model (4) leads to the following approximation for the dielectric constant, which can be used in an optical frequency range:

$$\varepsilon(\omega) = \frac{\beta}{\omega_b^2 - \omega(\omega - i\nu_b)}. \tag{6}$$

Formula (6) adequately reproduces the experimentally observed complex dielectric constant of bismuth [15] for $\omega_b = 1\times10^{15}$ s^{-1}, $\sqrt{\beta} = 9\times10^{15}$ s^{-1}, $\nu_b = 1\times10^{15}$ s^{-1}.

In the first approximation the monochromatic field (1), (2) causes oscillations of free and 'bound' electrons at a frequency ω_0. Because the movement of the surface carriers in a perpendicular-to-the-boundary direction is nonlinear, this leads to the formation of a low-frequency current.

3. Nonlinear current

The transverse component of the electric field E_x induces a charge near the surface of a semi-metal. The electrons localised near the boundary are displaced by the longitudinal electric field of laser radiation and excite a nonlinear surface current. For a quantitative description of this process, we consider the hydrodynamic equations in the representation of complex amplitudes. The change in the electron density n by the action of the laser field is found from the equation of continuity

$$i\omega_0 e\delta n = \operatorname{div} \boldsymbol{j}, \tag{7}$$

where $\boldsymbol{j} = -i\omega_0 e n_0 \boldsymbol{r}_f$; and n_0 is the unperturbed concentration of conduction electrons. It should be noted that the transverse component of the current $j_x(x)$ has a discontinuity at the bismuth–vacuum interface, which corresponds to a charge induced on the surface. At the same time, both components of the current in the skin layer produce a charge disturbance. Thus, the expression for the concentration disturbance is written in the form:

$$\delta n = -\frac{e n_0 \exp(-ik_z z)}{\omega_0^2 - i\nu_f\omega_0}\left\{\frac{E_x|_{x=0}}{m_x}[-\delta(x) - ik_x\exp(-ik_x x)] - ik_z\exp(-ik_x x)\frac{E_z|_{x=0}}{m_z}\right\}, \tag{8}$$

where $k_x = k_0\sqrt{-\varepsilon}$; and $k_z = k_0\cos\alpha$. A longitudinal low-frequency current can be obtained by averaging the product of concentration and longitudinal velocity of the electrons with respect to the optical period. Below, we will consider only the longitudinal nonlinear current, because this current makes a major contribution to the emission from the surface of bismuth with configurations of effective masses (i.e., crystal orientations), corresponding to a maximum efficiency of THz generation.

Substituting the values of electric fields on the surface of bismuth in expression (8), after averaging we finally obtain the expression for the longitudinal current density in the skin layer:

$$j_{z\,\mathrm{THz}} = -\frac{e^3|E_0|^2 n_0 \sin^2\alpha\,|1-R|^2\exp(2x\operatorname{Im}k_x)}{2cm_z(\omega_0^2+\nu_f^2)} \times\left\{\frac{1}{m_x}\left[\delta(x)\frac{\operatorname{Im}k_x}{k_0^2|\varepsilon(\omega_0)|} - 1\right] + \frac{1}{m_z}\right\}. \tag{9}$$

Integrating (9) over the skin depth, we find an expression for the surface current:

$$J_{\mathrm{surf}} = -\frac{e^3 |E_0|^2 n_0 \sin^2\alpha \cos\alpha\, |1-R|^2}{4cm_z(\omega_0^2+\nu_{\mathrm{f}}^2)\,\mathrm{Im}\,k_x}$$

$$\times\left\{\frac{1}{m_x}\left[\frac{(\mathrm{Im}\,k_x)^2}{k_0^2|\varepsilon(\omega_0)|}-1\right]+\frac{1}{m_z}\right\}. \quad (10)$$

In the case of a femtosecond laser pulse, whose wavelength is much smaller than its transverse dimension, nonlinear current will appear in the region of the overlap of incident and reflected optical radiation propagating along the surface of the semi-metal. The temporal current waveform (10) is determined by the envelope of the laser pulse.

The surface current J_{surf}, 'running' with a superluminal velocity along the vacuum–semi-metal interface (a medium with a large modulus for ε) excites a system of volume low-frequency currents inside the material. We assume that the current is produced by the obliquely incident laser pulse with a sufficiently large transverse dimension, so that the value of J_{surf} depends only on the running coordinate $\xi = t - (z\cos\alpha)/c$. This geometry corresponds to typical experimental conditions in the generation of THz radiation on the surface of a metal [2–4, 8]. Because the speed of movement of the source is greater than the speed of light, the produced radiation is of Cherenkov type.

4. Electromagnetic radiation of the surface current

Consider the solution of the problem of radiation of the found surface current. To describe the emission, we write Maxwell's equations with a surface current source $\boldsymbol{S}(t)$:

$$\frac{\partial \boldsymbol{H}}{\partial t} = -c\,\mathrm{rot}\boldsymbol{E}, \quad (11)$$

$$\frac{\partial \boldsymbol{E}}{\partial t} = c\,\mathrm{rot}\boldsymbol{H} - 4\pi\frac{\partial \boldsymbol{P}}{\partial t} - 4\pi\boldsymbol{j}, \quad (12)$$

$$\frac{\partial^2 \boldsymbol{P}}{\partial t^2} + \nu_{\mathrm{b}}\frac{\partial \boldsymbol{P}}{\partial t} + \omega_{\mathrm{b}}^2\boldsymbol{P} = \beta\boldsymbol{E}, \quad (13)$$

$$\frac{\partial \boldsymbol{j}}{\partial t} + \nu_{\mathrm{f}}\boldsymbol{j} = e^2\hat{M}_{\mathrm{f}}^{-1}n_0\boldsymbol{E} + \boldsymbol{S}(t)\delta(x). \quad (14)$$

Turning to the problem of finding the fields of the Cherenkov radiation, we make a substitution $z \to z - Vt$ ($c/\cos\alpha = V$) and seek a stationary solution ($\partial/\partial t = 0$). Taking into account the value of the dielectric constant of bismuth, so as not to make the calculations cumbersome, we can neglect the left-hand side in equation (12). Then, we obtain a system of equations for the electromagnetic fields inside bismuth ($-L < x < 0$):

$$\frac{V}{c}\frac{\partial H_y}{\partial z} = \frac{\partial E_z}{\partial x}, \quad (15)$$

$$\frac{\partial H_y}{\partial x} = 4\pi\frac{V}{c}\frac{\partial P_z}{\partial z} + \frac{4\pi}{c}j_z, \quad (16)$$

$$V^2\frac{\partial^2 P_z}{\partial z^2} + \nu_{\mathrm{b}}V\frac{\partial P_z}{\partial z} + \omega_{\mathrm{b}}^2 P_z = \beta E_z, \quad (17)$$

$$V\frac{\partial j_z}{\partial z} + \nu_{\mathrm{f}}j_z = \frac{e^2}{m_z}n_0 E_z. \quad (18)$$

The system contains no equations for the transverse components, i.e., by excluding the term $(\partial E_x/\partial z)$ in equation (11), the system is closed. After calculating the radiation fields we go back to the conditions of applicability of the approximations made.

On the bismuth surface (in the vicinity of $x = 0$), we have an expression for the current density

$$V\frac{\partial j_z}{\partial z} + \nu_{\mathrm{f}}j_z = S(z/V)\delta(x). \quad (19)$$

Passing in (15)–(18) to the Fourier representation along the z coordinate and solving the resulting system with respect to the magnetic field, we obtain the equation

$$\frac{\partial^2 H_y}{\partial x^2} = -\chi H_y, \quad (20)$$

$$\chi = \frac{1}{c^2}\left(\frac{4\pi\beta V^2 k_z^2}{-V^2k_z^2 + \nu_{\mathrm{b}}Vik_z + \omega_{\mathrm{b}}^2} - \frac{4\pi e^2 n_0}{m_0}\frac{Vik_z}{\nu_{\mathrm{b}} + Vik_z}\right), \quad (21)$$

where m_0 is the mass of a free electron.

Boundary conditions in the case of a bismuth layer occupying a region $-L < x < 0$ have the form:

$$H_y|_{x=-0} - H_y|_{x=+0} = \frac{4\pi}{c}J_{\mathrm{surf}}, \quad (22)$$

$$H_y|_{x=-L+0} - H_y|_{x=-L-0} = 0. \quad (23)$$

In vacuum, for the Cerenkov radiation field we can write the expressions

$$H_y|_{x=+0} = -\frac{E_z|_{x=0}}{\sin\alpha}, \quad (24)$$

$$H_y|_{x=-L-0} = \frac{E_z|_{x=-L}}{\sin\alpha}. \quad (25)$$

Inside bismuth, in accordance with the approximation made, the electric field is related to the magnetic field by the expression:

$$\frac{\partial H_y}{\partial x} = -\frac{c\chi}{Vik_z}E_z. \quad (26)$$

Using boundary conditions (22), (23) and the relations between the magnetic and electric fields at the bismuth–vacuum interface (24)–(26), taking into account the continuity of the longitudinal electric field E_z we can obtain a linear system of equations for the coefficients of the general solution for the magnetic field

$$H_y = A\exp(\mathrm{i}\sqrt{\chi}\,x) + B\exp(-\mathrm{i}\sqrt{\chi}\,x). \quad (27)$$

Solving this system of equations, we obtain the expressions for the magnetic field above and below the layer of bismuth:

$$H_y|_{x=+0} = -\frac{1}{\sin\alpha}\frac{Vk_z}{c\sqrt{\chi}}(A - B), \quad (28)$$

$$H_y|_{x=-L-0} = \frac{1}{\sin\alpha}\frac{Vk_z}{c\sqrt{\chi}}[A\exp(\mathrm{i}\sqrt{\chi}L) - B\exp(-\mathrm{i}\sqrt{\chi}L)], \quad (29)$$

where

$$A = \frac{4\pi}{c}\frac{J_{\text{surf}}}{f_- - (f_+^2/f_-)\exp(2\mathrm{i}\sqrt{\chi}L)};$$

$$B = \frac{4\pi}{c}\frac{J_{\text{surf}}}{f_+ - (f_-^2/f_+)\exp(-2\mathrm{i}\sqrt{\chi}L)};$$

$$f_\pm = 1 \pm \frac{k_z V}{c\sqrt{\chi}\sin\alpha}.$$

Returning to the conditions of applicability of the approximation used in equation (11), we note that the expression for the transverse component of the vector equation (12), by analogy with (26), yields the relation

$$E_x \sim \frac{c}{V}\frac{k_z^2 H_y}{\chi}. \tag{30}$$

It follows that

$$\frac{\partial H_y}{\partial z} = \frac{V}{c}\frac{\partial E_z}{\partial x} \gg \frac{V}{c}\frac{\partial E_x}{\partial z}.$$

In the case of the half-space occupied by bismuth, the above solution corresponds, with an accuracy up to small corrections, to the general solution from papers [7, 8]

$$E_z = \frac{4\pi}{c\sqrt{-\varepsilon_{\text{THz}}}} j_{\text{surf}}, \tag{31}$$

where ε_{THz} is the dielectric constant in the THz frequency range. The magnetic field above the metal surface (in vacuum) can be determined from Maxwell's equations:

$$H_y = \frac{E_z}{\sin\alpha}. \tag{32}$$

The low-frequency radiation energy flux per unit area (i.e. the normal component of the Poynting vector) has the form

$$S_x = \frac{c}{4\pi} E_z H_y^* = \frac{4\pi}{c\,|\varepsilon_{\text{THz}}|\sin\alpha}|j_{\text{surf}}|^2. \tag{33}$$

For evaluation, we assume that the incident optical pulse has a Gaussian envelope along the radial coordinate and with respect to time, i.e. its intensity on the sample surface is proportional to

$$|E|^2 = E_0^2 \exp\left(-\frac{y^2}{a^2} - \frac{z^2}{a_z^2} - \frac{\xi^2}{T^2}\right), \tag{34}$$

where a is the transverse size of the laser beam; T is the laser pulse duration with $cT \ll a$; and $a_z = a/\sin\alpha$. In accordance with the condition of Cherenkov synchronism, the low-frequency radiation will propagate in the direction of specular reflection of the laser beam. Integrating the energy flux (33) over time and surface area, we can calculate the total energy radiated in the form of a low-frequency pulse upon reflection of optical radiation from the semi-metal:

$$W_{\text{Bi}} \simeq \frac{e^6 E_0^4 n_0^2}{c\,|\varepsilon|\,\omega_0^6} a^2 T \left(\frac{0.77}{m_x m_z} + \frac{1}{m_z^2}\right)^2 \times \frac{\sin^2\alpha\cos^2\alpha}{(1 + 4\sin\alpha + 29\sin^2\alpha)^2}. \tag{35}$$

As can be seen from formula (35), the energy of the low-frequency response must strongly depend on the single crystal orientation (which determines the value of the effective masses m_z and m_x).

The above-obtained analytical results were compared with the numerical solution of the Cauchy problem describing the incidence and reflection of the laser pulse, the formation of low-frequency nonlinear currents and their radiation in the form of THz pulses. The simulation runs until a steady state corresponding to the Cerenkov radiation is reached. This allows one to exclude the switching/transition effects (for details, see the Appendix). The simulation results for the angle of incidence $\alpha = 33.5°$ are shown in Fig. 1. In the numerical simulation we used quite a thin layer of bismuth with a thickness of $\lambda_0/3$, where λ_0 is the wavelength of the optical pulse.

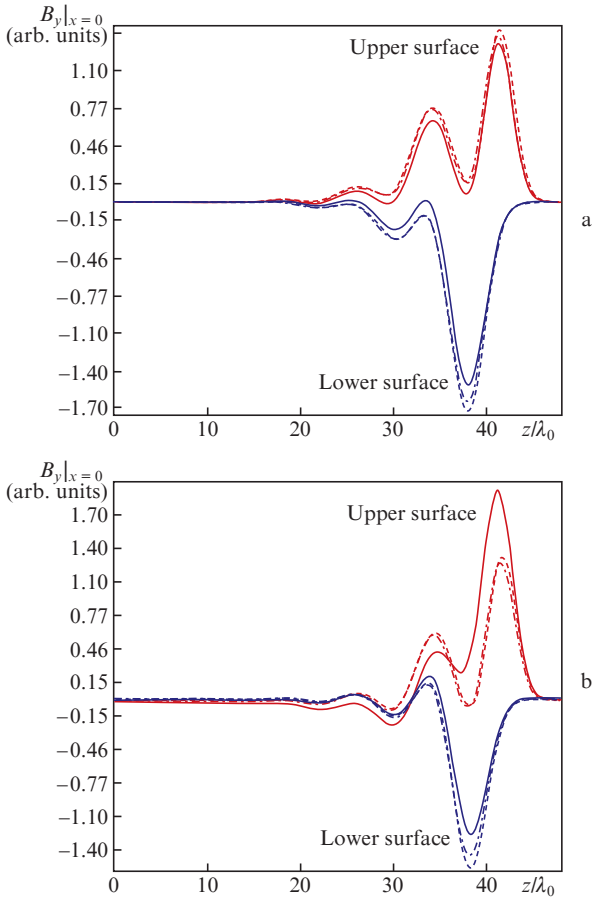

Figure 1. Shape of the emitted THz signal from the upper and lower surfaces of a bismuth plate having a finite thickness for (a) $m_0/m_x = 3.84$, $m_0/m_z = 1000$ and (b) $m_0/m_x = 200$, $m_0/m_z = 1000$. The solid curves show the results of numerical simulation of the complete system of nonlinear hydrodynamic equations, the dashed curves correspond to the analytic solution, and dot-and-dash curves – to numerical simulation with a given tangential current source (7).

Table 1. THz radiation energy (in rel. units) for various combinations of effective masses of the electron in the x and z axes, obtained by numerical simulation within the framework of the complete system of hydrodynamic equations of the electron gas. A plate of finite thickness is considered, and THz signals from the upper and lower surfaces are summarised.

m_0/m_z	m_0/m_x		
	3.84	200	1000
3.84	–	1.15×10^{-5}	2.15×10^{-3}
200	3.3×10^{-3}	–	3.12×10^{-1}
1000	1.88	2.25	–

The best agreement of the numerical solution with the analytical one for the emitted low-frequency field is achieved at the greatest transverse effective mass of the electrons. In this case, radiation can be described only by longitudinal currents. Table 1 shows the calculated generation efficiency for different positions of the axes of the crystal with respect to the plane of incidence. It can be seen that the highest generation efficiency is achieved when the smallest effective mass of the electrons corresponds to the direction determined by the intersection of the plane of incidence with the sample surface.

Let us compare the energy of low-frequency radiation (35) for bismuth with the energy of radiation from the the surface of a highly conductive metal (gold, copper, aluminium, etc.). At an optimal angle of incidence of the laser pulse on the metal, the total energy of the THz response caused by the instantaneous quadratic nonlinearity is described by the expression [7]:

$$W_{\rm m} = \frac{9}{32}\sqrt{\pi/2}\,\frac{e^2}{m_0^2}\,\frac{a^2}{\omega_0^2\omega_{\rm m}^2 cT}\,E_0^4, \tag{36}$$

where $\omega_{\rm m}$ is the plasma frequency of the electrons in the metal. The ratio of energies (35) and (36) for the characteristic plasma frequency of the metal, $\omega_{\rm m} \simeq 20-30$ fs^{-1}, at a laser pulse duration of 50 fs is

$$\frac{W_{\rm Bi}}{W_{\rm m}} \simeq 10^4. \tag{37}$$

Thus, one should expect a significant increase in the energy of the generated low-frequency radiation in the transition to semi-metals due to a significant decrease in the effective mass of an electron in the crystal. In addition, the degree of shielding of optical and low-frequency radiation inside a semi-metal (proportional to $|\varepsilon|^{-3}|\varepsilon_{\rm THz}|^{-1}$) may be less than in a normal metal [where it is proportional to $(\omega_{\rm m}T)^{-2}$].

5. Conclusions

In this paper we have proposed a theoretical model of generation of THz radiation when the surface of the semi-metal is irradiated by a femtosecond laser pulse. The mechanism in question is a generalisation of the mechanism of an instantaneous quadratic response of a metal, analysed in [5, 7].

It is shown that the transition from highly conductive metals to semi-metals can be accompanied by a significant increase in the amplitude of the low-frequency response (37) due to a reduction in the effective mass of the charge carrier and weakening of shielding of electromagnetic fields. In addition, the model predicts a strong dependence of the THz signal energy on the effective masses of the electron in x and z directions (35), i.e. on the orientation of the single-crystal sample.

Acknowledgements. The authors thank V.Ya. Aleshkin, A.M. Satanin and A.A. Balakin for useful discussion of the material in this paper and assistance in the preparation of the manuscript.

This work was supported by the Russian Foundation for Basic Research (Grant Nos 16-32-00717, 16-02-01078 and 14-22-02034).

Appendix. Numerical simulation

For the numerical calculation of the problem of THz pulses, we have modified the approach previously developed for metals in [7]. In this approach, the Cauchy problem is calculated with a source simulating the incidence of an optical plane wavefront pulse onto the surface. The calculation is performed until the Cherenkov radiation reaches a steady state. In numerical simulations, account is taken of both the hydrodynamic nonlinearities emerging from the term $(\boldsymbol{v}\nabla)\boldsymbol{v}$ and the nonlinearities associated with the magnetic field and with the inhomogeneity of the concentration of free charge carriers arising under the action of the laser field. In this case, the presence of the electron gas temperature $T_{0\rm eff}$ corresponding to the Fermi energy in bismuth is also taken into account. For the influence of bound electrons to be taken into account, the model [7] has been supplemented with the equation describing the polarisation:

$$\frac{\partial \boldsymbol{H}}{\partial t} = -c\,{\rm rot}\boldsymbol{E},$$

$$\frac{\partial \boldsymbol{E}}{\partial t} = c\,{\rm rot}\boldsymbol{H} - 4\pi\frac{\partial \boldsymbol{P}}{\partial t} - 4\pi\boldsymbol{j},$$

$$\frac{\partial^2 \boldsymbol{P}}{\partial t^2} + \nu_{\rm b}\frac{\partial \boldsymbol{P}}{\partial t} + \omega_{\rm b}^2\boldsymbol{P} = \beta\boldsymbol{E},$$

$$\frac{\partial n}{\partial t} = -\frac{1}{e}\,{\rm div}\boldsymbol{j},$$

$$\frac{\partial \boldsymbol{j}}{\partial t} + \nu_{\rm f}\boldsymbol{j} = \frac{1}{n}[(\boldsymbol{j}\nabla)\boldsymbol{j} - \boldsymbol{v}{\rm div}\boldsymbol{j}] + e^2\hat{M}_{\rm f}^{-1}n\boldsymbol{E}$$

$$+ \frac{e}{c}\hat{M}_{\rm f}^{-1}\boldsymbol{j}\times\boldsymbol{B} + T_{0\rm eff}\nabla n,$$

where $\boldsymbol{v}$ is the velocity of the ordered motion of free electrons.

The second equation of hydrodynamics for the current of free electrons has been modified by introducing an anisotropic mass of free carriers described by the effective mass tensor $\hat{M}_{\rm f}$. The system was solved in the same manner as in [7]. The equation for the polarisation was integrated implicitly. Rewriting (4) in the form of an ordinary differential equation of first order for the vector $(\boldsymbol{P}, \boldsymbol{Q})$, where $\boldsymbol{Q} = \dot{\boldsymbol{P}}$, and using the values of these quantities at different times: $\boldsymbol{p}_i = \boldsymbol{P}(t_i)$, $\boldsymbol{q}_i = \boldsymbol{Q}(t_i - {\rm d}t/2)$, we obtain the algebraic system:

$$\boldsymbol{q}_{i+1} - \boldsymbol{q}_i + \frac{\nu_{\rm b}}{2}(\boldsymbol{q}_{i+1} + \boldsymbol{q}_i){\rm d}t = (-\omega_{\rm b}^2\boldsymbol{p}_i + \beta\boldsymbol{E}_i){\rm d}t,$$

$$\boldsymbol{p}_{i+1} - \boldsymbol{p}_i = \boldsymbol{q}_{i+1}{\rm d}t.$$

One can see that the quantities $\boldsymbol{p}_{i+1}$ and $\boldsymbol{q}_{i+1}$ can be explicitly calculated from the values of $\boldsymbol{p}_i$ and $\boldsymbol{q}_i$. The calculation of $\boldsymbol{q}_{i+1}$ was conducted before calculating the electric field $\boldsymbol{E}_{i+1} = \boldsymbol{E}(t_i + {\rm d}t)$.

References

1. Hilton D.J., Averitt R.D., Meserole C.A., et al. *Opt. Lett*., **29**, 1805 (2004).
2. Kadlec F., Kuzel P., Coutaz J.-L. *Opt. Lett*., **29**, 2674 (2004).
3. Kadlec F., Kuzel P., Coutaz J.-L. *Opt. Lett*., **30**, 1402 (2005).
4. Suvorov E.V., Akhmedzhanov R.A., Fadeev D.A., et al. *Opt. Lett.*, **37**, 2520 (2012).
5. Uryupin S.A., Frolov A.A. *Zh. Eksp. Teor. Fiz*., **141**, 1006 (2012).
6. Uryupin S.A., Frolov A.A. *Kvantovaya Elektron*., **44** (9), 866 (2014) [*Quantum Electron*., **44** (9), 866 (2014)].
7. Mironov V.A., Oladyshkin I.V., Suvorov E.V., Fadeev D.A. *Zh. Eksp. Teor. Fiz*., **146** (2), 211 (2014).
8. Akhmedzhanov R.A., Ilyakov I.E., Mironov V.A., Oladyshkin I.V., Suvorov E.V., Fadeev D.A., Shishkin B.V. *Izv. Vyssh. Uchebn. Zaved., Ser. Radiofiz*., **57** (11), 902 (2014).
9. Oladyshkin I.V., Fadeev D.A., Mironov V.A. *J. Opt.*, **17**, 075502 (2015).
10. Agranovich V.M., Mills D.D. (Eds) *Surface Polaritons: Electromagnetic Waves at Surfaces and Interfaces* (Amsterdam: Elsevier, 1982; Moscow: Nauka, 1985).
11. Mamonov M.A., Prudnikov V.V., Prudnikova I.A. *Fizika poverkhnosti. Teoreticheskie modeli i eksperimental'nye metody* (Surface Physics. Theoretical Models and Experimental Methods) (Moscow: Fizmatlit, 2011).
12. Oladyshkin I.V. *Pis'ma Zh. Eksp. Teor. Fiz*., **103**, 495 (2016).
13. Fal'kovskii L.A. *Usp. Fiz. Nauk*, **94**, 3 (1968).
14. Edel'man V.S. *Usp. Fiz. Nauk*, **123**, 257 (1977).
15. Madelung O. *Semiconductors: Data Handbook* (New York: Springer-Verlag, 2003).
16. Landau L.D., Lifshitz E.M. *Electrodynamics of Continuous Media* (Oxford: Pergamon Press, 1984; Moscow: Nauka, 1982).